

EFFECT OF VACUUM ON HIGH-TEMPERATURE DEGRADATION OF GOLD/ALUMINUM WIRE BONDS IN PEMs

Alexander Teverovsky
QSS Group, Inc.
GSFC/NASA, Code 562, Greenbelt, MD 20771
Alexander.A.Teverovsky.1@gsfc.nasa.gov

ABSTRACT

Gold/aluminum wire bond degradation is one of the major failure mechanisms limiting reliability of plastic encapsulated microcircuits (PEMs) at high temperatures. It is known also that oxidative degradation is the major cause of failures in epoxy composite materials; however, the effect of oxygen and/or vacuum conditions on degradation of PEMs has not been studied yet.

In this work, three groups of linear devices have been subjected to high-temperature storage in convection air chambers and in a vacuum chamber. Electrical characteristics of the devices, variations of the wire bond contact resistances, mass losses of the packages, and thermo-mechanical characteristics of the molding compounds were measured periodically during the testing. The results showed that high-temperature storage in vacuum and air conditions changed thermo-mechanical characteristics of molding compounds in a similar way; however, the failure rates and the degree of wire bond degradation for parts stored in air was significantly larger than for parts stored in the vacuum chamber.

A mechanism of Au/Al wire bond failures in PEMs at high temperatures, the role of oxygen, and non-linearity of the degradation rate at a certain critical temperature above the glass transition temperature of molding compounds are discussed.

1. INTRODUCTION

Gold wires have been widely used for interconnection between aluminum contact pads in silicon dice to silver-plated copper, or alloy 42, lead frames in the production of commercial microcircuits for more than 30 years. Reliability of the interconnection has been a subject of multiple investigations for all these years, which has led to understanding of many aspects of the Au/Al wire bond (WB) reliability [1].

The generally accepted mechanism of WB degradation at high temperatures includes interdiffusion reactions resulting in formation of multiple Au/Al intermetallic compounds. This process stabilizes when all Al metallization under the bond is consumed and the intermetallic eventually transfers into a gold-rich Au₄Al composition [2]. At 175 °C, Al transformation into the Al₂Au phase was observed already after 2 hrs., and after approximately 10 hrs. all aluminum metallization was completely consumed. The transformation into the gold-rich phase starts after approximately 50 hrs. at 175 °C and

finishes after ~150 hrs. resulting in the formation of intermetallic compound layers of 2 to 4 μm in thickness. At 250 °C it takes ~30 min. to complete these transformations. Phase transformations lateral to the WB proceed concurrently the conversions of Au/Al compounds across wire bonds, but these require more time to complete.

Intermetallic growth and transformations occur along with formation of voids inside the bonds at the gold/intermetallic interface and in aluminum contact pads along the periphery of the bonds. The voids are a result of coalescence of vacancies formed due to the difference between the diffusion rates of Al and Au atoms (Kirkendall effect). The formation of the intermetallics makes the bonds stronger, but more brittle and mechanically stressed due to volumetric change in the intermetallics compared to Au and Al [1, 3]. Electrical resistance of the wire bonds increases due to intermetallic formation on only a few dozen milliohms [1, 4]. During the initial stages of the degradation, voiding does not affect the mechanical strength and contact resistance of the bonds significantly. However, prolonged high-temperature exposure increases the voiding to the point at which the bond becomes mechanically weak and/or the electrical resistance increases above the acceptable level, thus causing failure of the devices.

For plastic encapsulated microcircuits, the WB degradation process is complicated due to mechanical stresses in the package and to release of corrosive molecules from molding compound, MC. Most currently used MCs employ brominated epoxies to provide flame resistivity to the plastics. Thermal decomposition of these epoxy materials, and flame-retardant additives in particular, results in formation of multiple chemically active molecules. These include halides such as methyl bromide (H₃C-Br) and hydrogen bromide (HBr), water, carbon oxides, and other molecules with low molecular weight, which can react with the Al/Au intermetallics causing dry corrosion of the bond [5, 6, 7]. Uno and Tatsumi [7] have shown recently that the corrosion of intermetallic compounds is specific to the Au₄Al phase and does not occur on Au₂Al and Au₅Al₂ compositions.

Antimony trioxide (Sb₂O₃) is commonly added to MCs as a synergist to increase the efficiency of brominated flame retardants. Gallo [8] has shown that at high temperatures the presence of this synergist also causes corrosion of intermetallic compounds in WBs and that the antimony trioxide has an overriding effect compared to brominated epoxy.

Resulting from the directive of William Perry, former Secretary of Defense, in June 1994, in recent years an increasing proportion of commercial-off-the-shelf (COTS) devices encapsulated in plastic packages with Au/Al interconnections are being used in military and aerospace applications. Insertion of these devices into high-reliability systems necessitates rigorous screening and qualification testing, which are based on application of accelerated high-temperature stresses. This requires better understanding of WB degradation mechanisms to adequately evaluate the quality of WBs and predict reliability of parts in specific applications, including vacuum conditions for space systems.

It has been shown that environmental conditions, and in particular the presence of moisture, significantly affect degradation of wire bonds in PEMs, so the failures can be observed already after a few hundred hours during highly accelerated stress testing (HAST) at 85% RH and temperatures from 130 to 150 °C [9]. It is also known that at high temperatures oxidative degradation is the major cause of failures in epoxy composite materials [10]; however, the effect of oxygen and/or vacuum conditions on degradation of PEMs has not been studied yet.

In this work, three groups of linear devices encapsulated in plastic SOIC-8-type packages have been subjected to high-temperature storage (HTS) testing in air and vacuum conditions. Characteristics of the molding compounds and electrical characteristics of the devices were measured periodically during the testing. Test results and analysis of failed devices indicated a significant role of oxygen in the high-temperature degradation processes in PEMs and allowed for elaboration of the WB degradation mechanism.

2. EXPERIMENTAL PROCEDURE

2.1. Parts used.

Three types of commercial plastic encapsulated devices, a dual operational amplifier (OP), and two types of precision bandgap voltage reference microcircuits (referred below as AD and LT) were used in this study. All parts were packaged in SOIC-8-style packages. Both voltage reference microcircuits had a thin layer of silicone gel coating on the die surface.

2.2. Testing of molding compounds.

Thermo-gravimetric analysis (TGA) was used to evaluate the thermal stability of molding compounds by monitoring mass losses of the packages as a function of time while temperature was increased linearly. The measurements were carried out using a TA2950 analyzer, TA Instruments, at a heating rate of 10 °C/min. from room temperature to 700 °C under the standard nitrogen purging conditions. Mass losses during isothermal aging were measured directly on the packages using a balance with an accuracy of 0.1 mg.

Thermo-mechanical analysis (TMA) is typically employed for measurements of the glass transition temperature (T_g) and coefficients of thermal expansion (CTE) in molding compounds by monitoring the deformation of a sample with temperature. In this work, the thermo-mechanical characteristics of encapsulating materials were measured directly on plastic packages using a thermal mechanical analyzer, TMA2940, TA Instruments, at a rate of 3 °C/min. during cooling from 220 °C followed by heating the part in the analyzer at the same rate. It has been shown [11] that this procedure allows for elimination of possible errors related to the presence of moisture and built-in mechanical stresses.

A PRISM200 detector and the Spirit software, developed by Princeton Gamma-Tech, were used to carry out X-ray microanalysis and evaluate the composition of flame retardants used in the molding compounds.

2.3. Contact resistance measurements.

Different techniques have been used by various researchers to measure contact resistance of the wire bonds (R_c). The values of R_c were measured using a special test structure in [4], or directly in microcircuits using measurements of the digital output voltage levels (VOL) under different load conditions [8].

In this work, variations of R_c due to stress testing were calculated based on measurements of the forward voltage drop (VF) of P-N junctions used in the input/output ESD protection circuits in the devices. To calculate R_c variations, the measurements were carried out before the stress [VF(0)] and after the stress [VF(t)] at a constant forward current (IF):

$$\delta R_c(t) = [VF(t) - VF(0)] / I_F$$

This technique does not require special test structures and allows for characterization of the WB quality directly on PEMs using both input and output pins, even on complex devices, without development of special programs for ATE to measure electrical characteristics of the part.

At $I_F = 5$ mA, the values of VF(0) were 0.7 to 0.9 V, which could be measured easily with an accuracy of 0.1 mV. Measurements have shown that the K-factor for these devices (the slope of VF variations with temperature) was in the range from 1.1 to 1.6 mV/°C. Considering possible temperature variations during measurements of ± 0.5 °C, the temperature-related variations of the R_c would be ~ 0.2 to 0.3 Ohm. The initial values of R_c are in the milliohm range and the observed stress-related variations were in the ohms range, so it can be assumed with relatively high accuracy that $\delta R_c(t) \approx R_c(t)$.

Electrical measurements of the devices after aging showed a good correlation between the results of R_c calculations using the forward voltage drop technique and the calculations based on electrical measurements of the output voltages under different load conditions.

The total number of WBs measured in each group during the HTS testing varied from 52 to 105.

2.4. High-temperature storage testing.

Two groups of each part type (16 to 30 samples in each group) were stored at 210 °C in a convection air chamber and in a vacuum (~ 0.5 torr) chamber for up to 1500 hrs. The characteristics of molding compounds and electrical characteristics of the parts were measured at various time intervals: after 120, 210, 350, 530, 700, 1000, and 1500 hours of HTS. Measurements of electrical characteristics of the devices and the contact resistances of WBs were carried out using a precision semiconductor parameter analyzer hp1456A.

To evaluate temperature dependence of WB degradation, in a separate set of experiments OP and AD microcircuits were stored in air convection chambers at 175, 190, 200, and 225 °C. Electrical characteristics of the parts and WB contact resistances were monitored periodically through these tests.

3. CHARACTERIZATION OF MOLDING COMPOUNDS

All parts used had the same package style; however, different materials were used for the lead frames and molding compounds. Table 1 shows thermo-mechanical characteristics, coefficients of thermal expansion in glassy (CTE1) and rubbery (CTE2) states, and glass transition temperatures of the molding compounds used.

Table 1. Characteristics of materials used in the parts design; average values and standard deviations (in brackets).

PN	LF CTE, ppm/°C	MC Tg, °C	MC CTE1, ppm/°C	MC CTE2, ppm/°C	Die coating
OP	17.5 (Cu)	166 (3)	17 (0.5)	86 (10)	-
AD	17.5 (Cu)	173 (5)	16.4 (1)	77 (25)	silicone
LT	4.3(A42)	138 (3)	9.8 (0.5)	75 (4.4)	silicone

The results indicate that a typical o-cresol novolac epoxy MC was used for OP and AD parts, whereas a low-Tg biphenyl type MC was used for the LT voltage reference microcircuits.

Results of TGA measurements for the three parts are shown in Figure 1 and indicate that the thermal stability of the MCs used in OP and AD parts was similar, but it was different from the MC used in LT parts.

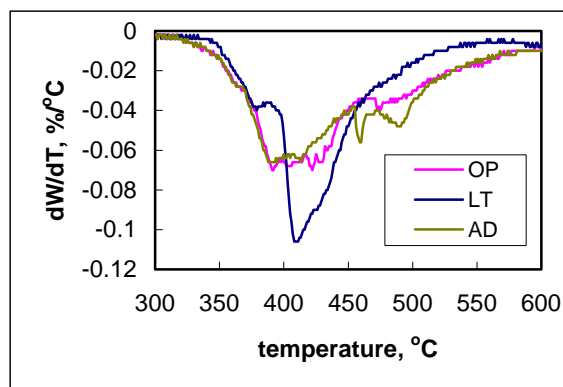


Figure 1. Differential TGA curves of the three plastic packages used.

Differential TGA chart for LT parts had two peaks at 383 °C and at 411 °C, indicating a two-stage decomposition process. The decomposition temperature (Td) was estimated at the onset of the increase of mass losses, at $dW/dT = 0.005\%/^{\circ}C$, and the temperature at the maximum weight loss rate (Tmax) was measured at the first peak value of the differential TGA chart. Results of these measurements are summarized in Table 2. These data indicate that the low-Tg MC used in LT parts had higher values of Td, thus confirming that the value of Tg is not an indicator of the thermal stability of MCs.

Table 2. Characteristics of thermal decomposition of molding compounds.

PN	Max rate, %/°C	Td, °C	Tmax, °C
OP	0.07	325	394
AD	0.066	325	394
LT	0.038	345	383

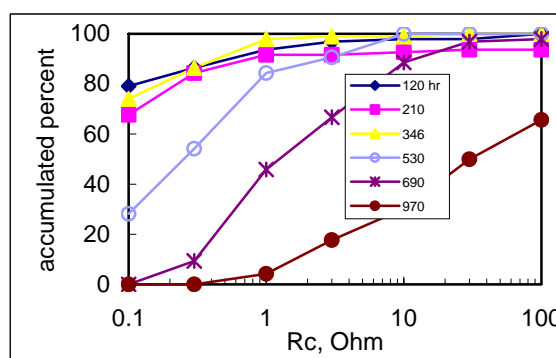
X-ray microanalysis has indicated the presence of bromine and antimony in all MCs, thus suggesting that all composites used

brominated epoxies and antimony trioxide synergist as flame retardants. Quantitative analysis has shown that all materials had similar concentration of Br (0.21 to 0.27 wt%). The concentration of Sb in the LT and AD devices was ~ 0.7 to 0.8 wt% and somewhat larger in the OP devices, ~1.4%.

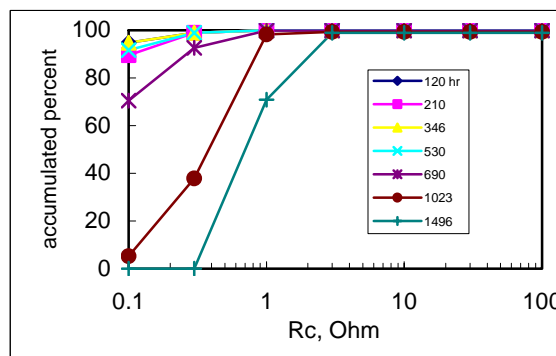
4. TEST RESULTS

4.1. Degradation of electrical characteristics.

Distribution of contact resistances at different times of storing of AD voltage reference microcircuits at 210 °C in vacuum and air chambers are shown in Figure 2. Noticeable variations in Rc were observed already after 120 hrs. for samples stored in air, whereas similar changes in parts stored in vacuum happened only after ~530 hours. After ~1000 hrs of air storage ~70% of WBs had Rc >10 Ohm, whereas all samples stored in vacuum conditions had Rc below 3 Ohm even after 1500 hrs. of the HTS testing.



a)



b)

Figure 2. Distributions of contact resistance of wire bonds at different times of storage of AD parts at 210 °C in air (a) and vacuum (b).

Figure 3 shows kinetics of median contact resistance values during the HTS testing in vacuum and in air chambers for LT and OP devices. All parts aged in air demonstrated significant increase in Rc (>1 Ohm) after 100 to 200 hrs and 50% of devices reached the 10 Ohm level after ~500 hrs., whereas in vacuum this level was not reached even after 1500 hrs. It is interesting to note that similar results were observed in [7] when WBs in parts stored at 200 °C increased their resistance to 10 Ohm after ~400 hrs.

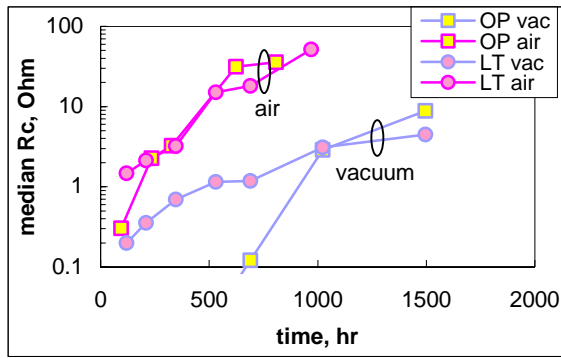


Figure 3. Kinetics of contact resistance variations during air and vacuum storage for OP and LT microcircuits.

In this work, an increase of the wire bond resistance to 10 Ohm was considered as a wire bond failure. Using this failure criterion, parameters of Weibull distributions (the characteristic life $[\tau_c]$ and the slope $[\beta]$) were calculated for all WB and parametric failures of the parts. Figures 4 and 5 give examples of these distributions for OP and LT microcircuits, and Table 3 summarizes results of these calculations.

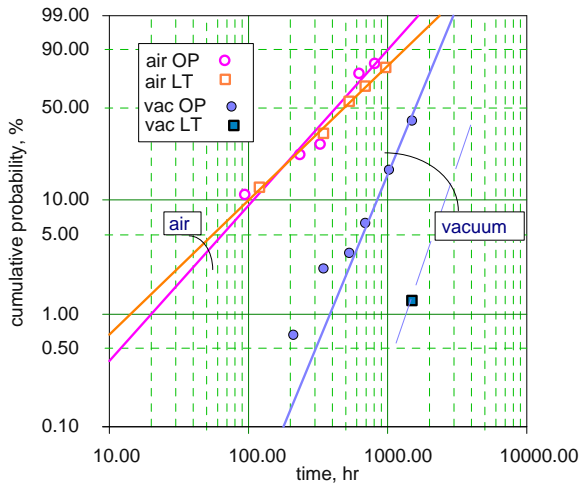


Figure 4. Cumulative probability for wire bond failures ($R_c > 10$ Ohm) during storage of OP and LT parts in air and vacuum chambers.

Analysis of the data indicates that the characteristic life of devices in vacuum is 3 to 8 times longer than in air conditions. A good correlation between the τ_c values calculated for the contact resistance failures and parametric failures of the parts suggests that for these microcircuits the wire bond degradation might be a limiting factor of reliability at high temperatures.

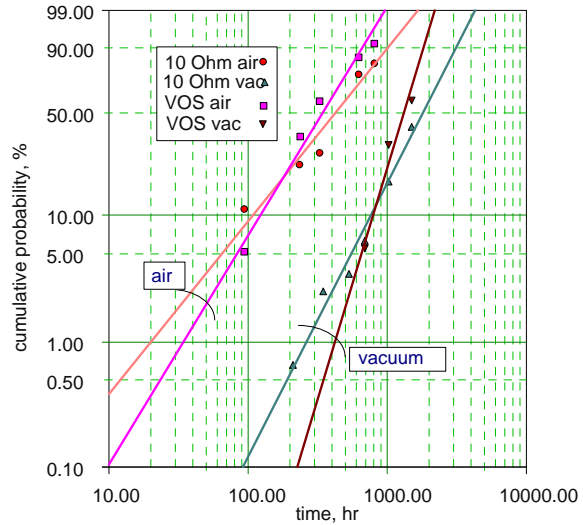


Figure 5. Cumulative probability for parametric failures (VOS) and wire bond failures ($R_c > 10$ Ohm) for operational amplifier microcircuits (OP) during air and vacuum storage.

Table 3. Characteristics of Weibull distributions for parametric and wire bond contact resistance failures.

Condition	OP		AD		LT	
	τ_c , hr	β	τ_c , hr	β	τ_c , hr	β
Param. air	419	1.84	800	2.25	791	2.21
Param. vac	1454	3.6	2750	2.25	3050*	3.6*
WB air	552	1.39	955	8.2	668	1.4
WB vac	1783	3	2647*	8*	5584*	3*

* Estimated parameters: the slope values were assessed by similarity and the τ_c values were calculated based on the first failure data.

No substantial difference was observed in reliability of voltage reference microcircuits encapsulated in high-Tg (AD) and low-Tg (LT) MCs, suggesting that the type of MC did not have an overriding effect on the WB reliability.

Degradation of the offset voltages (VOS) in operational amplifiers and output voltages (V_{out}), in the LT voltage reference microcircuits with time of storing in vacuum and air conditions is shown in Figures 6 and 7. Variations of these parameters during HTS in air were erratic and indicated multiple failures due to intermittent contacts, whereas parameters in devices stored in a vacuum chamber varied smoothly with time and had much fewer failures. In vacuum, the mean value of VOS increased on the average from $-90 \mu\text{V}$ to $+6 \mu\text{V}$ during the first 210 hrs. and then manifested good stability up to 1500 hrs. of HTS testing. The output voltages in LT microcircuits decreased smoothly with time of aging in vacuum conditions, saturating in the range of -400 ppm to -800 ppm after approximately 700 hrs. of storage.

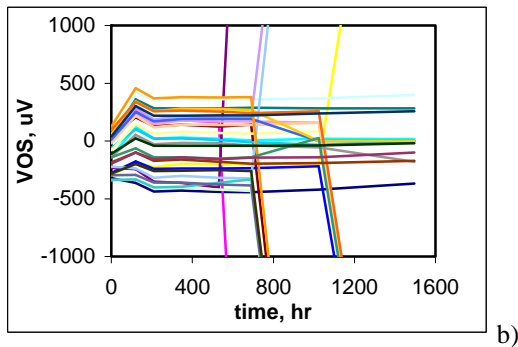
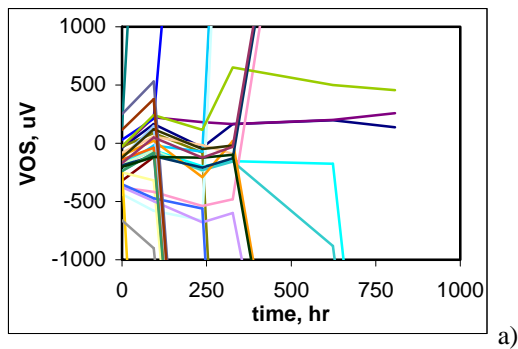


Figure 6. Variations of the offset voltages for operational amplifiers during high temperature storage testing in air (a) and vacuum (b) chambers.

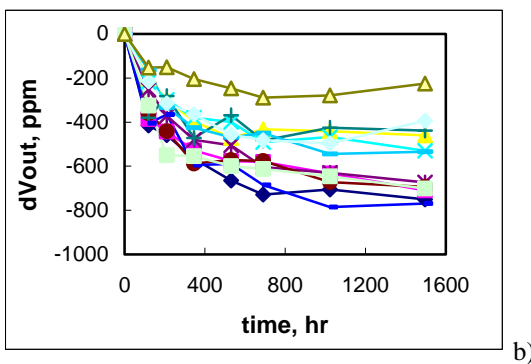
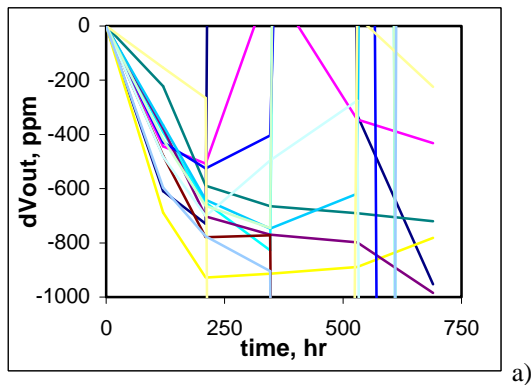


Figure 7. Output deviations of precision voltage reference microcircuits (LT) during HTS testing in air (a) and vacuum (b) chambers.

4.2. Degradation of molding compound.

Kinetics of mass losses of the parts during HTS is shown in Figure 8. After 1000 hrs. of aging, the mass losses in air were within the range of 1.1 to 1.4 % and continued to grow at a rate of 8×10^{-4} to 10^{-3} %/hr. The mass losses in vacuum were in the range of 0.2 to 0.45% and the rate of their variation was ~ 4 times less than in air. The mass losses in our calculations were rated to the total mass of the packages. Considering that for these devices the mass of MC is $\sim 50\%$ of the total mass of the packages, mass losses of MC would be approximately 2 times larger than those shown in Figure 8.

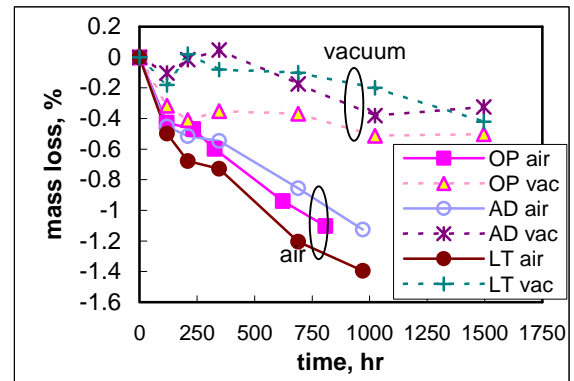


Figure 8. Average mass losses of the packages during high temperature storage at 210 °C.

The initial mass losses for OP devices (after 120 hrs. of HTS) were more significant than for other parts and similar for air ($\sim 0.41\%$) and vacuum ($\sim 0.37\%$) conditions, indicating that these parts had a higher concentration of low molecular weight contaminants. It is interesting that the LT parts, which had a minimal glass transition temperature, also had minimal mass losses, which corresponds to the TGA data and indicates that low-Tg materials do not necessarily have poor long-term stability at high-temperature conditions.

All specimens after air storage displayed a brownish tinge, whereas no change in appearance was observed in parts stored in vacuum conditions. These changes of color indicate oxidative degradation of molding compounds and are specific for the air-stored samples.

Figure 9 shows variation of the Tg and CTE caused by storage in air and vacuum conditions. For the LT parts, the values of Tg increased approximately 19 °C after vacuum aging and ~ 21 °C after air aging. For the high-Tg MCs (OP and AD devices), the Tg also increased in both environmental conditions; however, the changes were somewhat lesser: 7 to 12 °C in air and 10 to 12 °C in vacuum. No significant variations in the coefficient of thermal expansion, CTE1, of MC in AD and OP devices in both, vacuum and air conditions, were observed; however, the CTE1 in LT devices increased $\sim 70\%$ during HTS in vacuum. Similar increase in Tg values and some inconsistency in the CTE variations during HTS at temperatures from 170 to 260 °C for up to 1900 hrs. were observed also in [12].

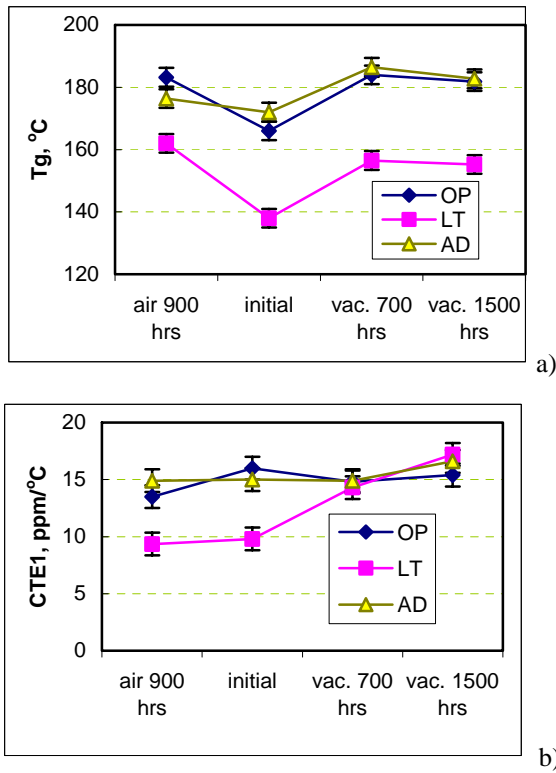


Figure 9. Effect of vacuum and air storage at 210 °C on the glass transition temperatures (a) and coefficients of temperature expansion in a glassy state (b) of molding compounds.

4.3. Temperature dependence of WB degradation in air.

To estimate the activation energy of failures during high-temperature storage in air, characteristics of Weibull distributions for parametric failures and WB resistance failures of OP and AD microcircuits were calculated based on the results of testing at temperatures from 175 to 225 °C. Figure 10 displays the temperature variation of the mean life for parametric and WB failures plotted in Arrhenius coordinates.

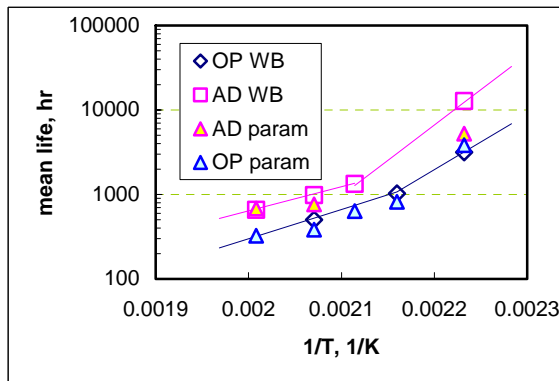


Figure 10. Arrhenius plots for mean life of parametric and wire bond failures OP and AD microcircuits tested in the range of temperatures from 175 °C to 225 °C.

Similar to what was observed before, the mean life calculated for parametric failures and contact resistance failures were close over the whole range of storage temperatures. The mean life curves indicated

different activation energies for low-temperature, below 190 to 200 °C, and high-temperature, 190 < T < 225 °C, regions. Results of the calculations are shown in Table 4 and indicate that in the high-temperature range the activation energies vary in a relatively narrow range from 0.55 to 0.67 eV; whereas at low temperatures the activation energy is much larger. This confirms the existence of a certain critical temperature, T_c , after which a mechanism of the wire bond degradation is changing, which corresponds to the observations made in [7, 13].

Table 4. Activation energies for OP microcircuits.

Temp. range	OP Param.	OP WB failures	AD WB failures
Low T	1.78	1.26	1.6
High T	0.68	0.67	0.55

4.4. Analysis of failed parts.

Typical acoustic microscopy images of the OP devices, after HTS testing in air and vacuum conditions, are shown in Figure 11. The results indicate extensive delaminations at the die surface along the periphery of the dice and at the finger-tips of the leads for the air-stored devices. The proportion of delaminations in the parts stored in vacuum was much lesser.

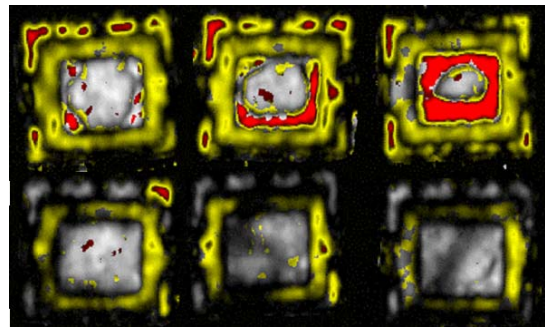


Figure 11. Examples of acoustic microscopy images for three OP microcircuits after storing at 210 °C for 700 hrs in air (top row) and in vacuum (bottom row) chambers.

Decapsulation of the parts in fuming nitric acid after air chamber storage took approximately 5 times longer than for the vacuum-stored parts, thus indicating significant structural changes in the polymer composites. Especially difficult to remove were the surface layers of the package, areas along the periphery of the die where delaminations were observed, and, in some cases, areas around the gold interconnecting wires.

Cross-sectioning of the devices after HTS in air (see Figure 12) revealed that discoloration in MCs existed not only along the surface of the package, but also in areas along the lead frame, die, and wire bonds. The thickness of the internal areas of discoloration was approximately the same as for the external layers. These areas of discoloration are most likely due to carbonization/charring of the molding compounds and they coincide with the areas that were difficult to remove during decapsulation. This indicates the existence of a free pass allowing air to reach internal areas of the package.

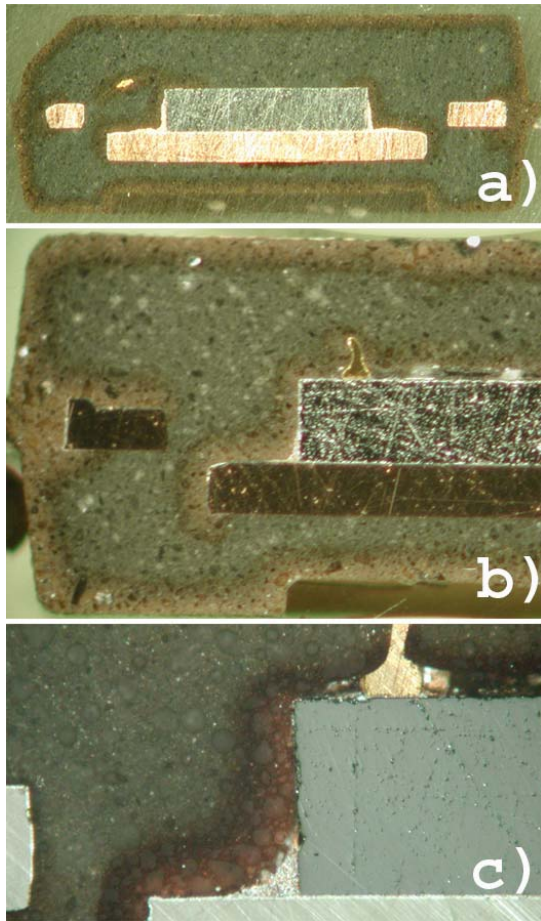


Figure 12. Cross-section of OP (a), AD (b), and LT (c) microcircuits after 900 hrs of storage in air at 210 °C.

Examples of optical images of the WB cross-sections in parts after 700 hrs. of aging are shown in Figure 13.

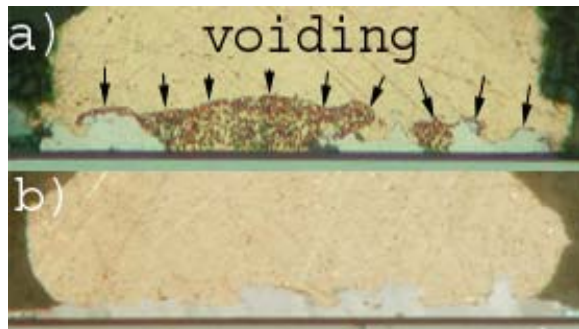


Figure 13. Cross section of wire bonds after 700 hrs. aging in air (a) and in vacuum (b). Note that extensive voiding in Au/Al intermetallic layers were observed only in the parts aged in air.

All samples stored in air experienced much more severe degradation of the bonds and manifested a lamellar structure, which is typical for corrosion of intermetallic compounds. EDS analysis of the intermetallics showed 95 to 97 wt% of Au and 5 to 3 wt% of Al, indicating a gold-rich phase close to the Au_4Al composition.

Typical SEM images of the bonds after HTS testing in air are shown in Figure 14. All wire bonds could be easily lifted, manifesting a porous structure of intermetallic compounds degraded

by the dry corrosion. The peripheral area of Al metallization around the bonds had multiple voids. In some cases, as in Figure 14b, their appearance suggested diffusion of Al atoms towards the WB along the crystalline grain boundaries in the Al metallization. In other cases, as in Figure 14c, the appearance of the voids suggested a corrosion attack, which affected mostly WB peripheral areas, but also was observed at some distance from the bonds. These cases were mostly characteristic of the LT microcircuits.

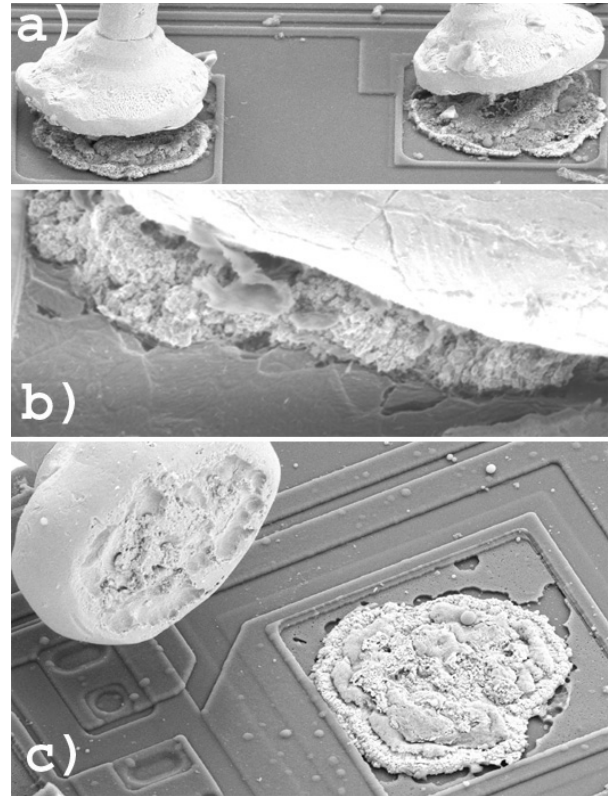


Figure 14. Wires broken along the Au/Al intermetallic compounds in OP (a), AD (b), and LT (c) microcircuits after 807 hrs of testing at 210 °C in air.

The appearance of wire bonds after vacuum aging is shown in Figure 15. In all, cases extensive intermetallic formation was observed; however, the level of degradation was less significant. Some WBs after vacuum aging remained intact and had the strength during the wire pull test of 4 to 6 g-f. Similar to what was observed after air storage, the appearance of aluminum contact pads in the LT devices after vacuum testing indicated corrosion attack of Al metallization (see Figure 16).

It is commonly assumed that the dry corrosion occurs mostly at the Au/Al intermetallic only and does not affect aluminum metallization. However, our data indicate that corrosion of Al metallization during HTS testing is possible. This type of corrosion might be due to excessive generation of methyl bromide in biphenyl compounds compared to o-cresol novolac epoxy compounds [7]. Methyl bromide, H_3C-Br , is known to be extremely aggressive towards aluminum forming methylaluminum sesquibromide, $(CH_3)_3Al_2Br_3$, which actively reacts with oxygen and/or water, and is spontaneously flammable in air.

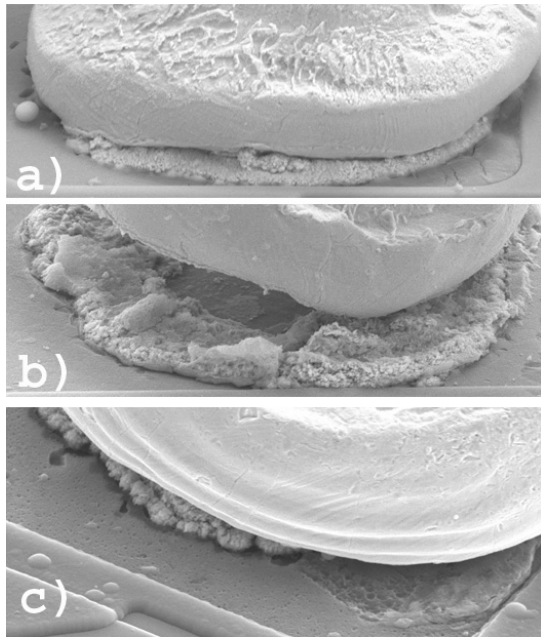


Figure 15. Wire bond degradation in OP (a), AD (b), and LT (c) microcircuits after 1500 hrs at 210 °C in vacuum chamber.

5. DISCUSSION

The results indicate significant reduction of WB failure rates during high temperature storage of the parts in vacuum compared to air conditions. To explain this, the role of oxygen in degradation processes of molding compounds and Au/Al wire bonds must be considered.

5.1. Thermal and thermo-oxidative degradation of molding compounds.

During high-temperature aging of polymers, the fluctuation of thermal energy might reach the point at which the polymer chain cleaves, separating two sigma-bonding electrons symmetrically and thus forming two radicals [14]. These radicals are chemically active and might recombine or react with another segment of the same polymer chain, causing chain scission or branching, or they might react with other molecules absorbed in the polymer, resulting in a complex process of chemical transformations.

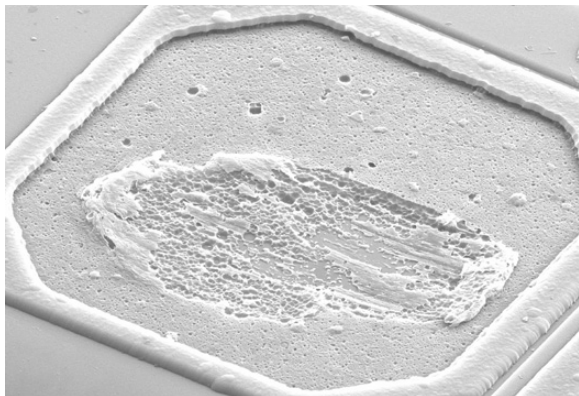


Figure 16. An example of corrosion of Al on an unbonded contact pad with a probe mark in the LT microcircuits after 1500 hrs at 210 °C in vacuum chamber.

In the presence of oxygen, radicals formed have a high probability of oxidation forming peroxides, which on dissociation produce two radicals, thus accelerating the degradation process [15]. This makes oxidative degradation the most common cause of failures of composite materials at high temperatures. The capability of oxygen to speed up decomposition of polymers has been used to develop a technique for accelerated thermo-oxidative degradation of composite materials at relatively low temperatures by using elevated pressures of oxygen [16].

The oxidative decomposition is considered to be a diffusion-controlled process and the oxygen concentration controls its rate. In our experiments (see Figure 12), the discoloration indicated charring in a surface layer of approximately 100 to 150 μm in thickness. Assuming that the thickness of this layer (L_d) is equal to the diffusion length of oxygen, the diffusion coefficient can be estimated as $D = L_d^2/t_s$, where t_s is the storage time at 210 °C. At $t_s \sim 900$ hrs., the calculation yields $D \sim 3.5 \times 10^{-11}$ cm²/s. This is an extremely low value considering that at room temperature diffusion coefficients of oxygen in different polymer materials vary from $\sim 10^{-8}$ to 10^{-5} cm²/s [17]. Due to exponential temperature dependence of diffusion coefficients in polymers, at 210 °C the value of D should be larger by several orders of magnitude.

This anomaly can be explained considering that the oxygen solubility in MC, rather than its diffusion rate, is the limiting factor of degradation of MCs in the presence of air. The thermo-oxidative process starts at the surface of MCs, where the concentration of oxygen is maximal. Decomposition and volatilization of the surface area result in mechanical stresses between the unaffected material and the degraded region, which has a reduced mechanical strength [16]. This results in the formation of a net of microcracks, thus providing an enhanced path for oxygen diffusion in the bulk of the polymer, promoting expansion of the cracks, and increasing the thickness of the degraded layer at the surface of the MC.

Discoloration of MCs along the lead frame (LF) top, and side surfaces of dice indicates the existence of a path for oxygen to freely access internal areas of the package. The formation of this path at temperatures exceeding T_g is due most likely to stress relaxation and to the difference in CTE values of the MC and lead frame. At normal conditions, when the temperature is below T_g , the lead frame/die assembly experience compressive stresses, and the MC is in intimate contact with the assembly. In this case, oxygen can reach the die only by diffusion through the bulk of the MC, and its concentration at the WBs depends on the solubility of oxygen in the polymer, which is relatively low. At temperatures close to T_g , the mechanical stresses are relaxing rapidly, and due to a large CTE in a rubbery state, at $T > T_g$ the MC expands significantly more than the lead frame, thus forming a gap. Neglecting the adhesion between MC and LF, a width of the gap, Δ , can be estimated as:

$$\Delta = (T - T_g) \times (CTE_{MC} - CTE_{LF}) \times L_{LF},$$

where L_{LF} is the thickness of the lead frame.

Assuming that to provide a free pass for air, the gap should be ~ 0.5 to 1 μm, a critical temperature (T_c), at which a sufficiently wide gap is created, can be estimated. At a thickness of the LF of 0.2 mm and $(CTE_{MC} - CTE_{LF}) \approx 70 \times 10^{-6}$ 1/°C, the necessary temperature should exceed T_g on 35 to 70 °C. This range is in agreement with our data, shown in Figure 10, where changes in the rate of WB and parametric failures occurred at ~ 190 °C, which is ~ 20 °C above T_g . These estimations are also in an agreement with the observations made [7, 13] in which changes in the activation energy of WB degradation were found to be on 40 to 60 °C higher than T_g . Obviously, an increase in T_g due to additional cross-linking at high

temperatures might reduce the difference between T_c and T_g on 15 to 20 °C.

It is interesting that delaminations along the periphery of the dice were detected by acoustic microscopy at room temperatures (see Figure 11). This is most likely due to decomposition and removal of a part of the MC in the air-accessible areas inside the package during HTS testing.

High-temperature storage of epoxy compounds might result in the scission of polymer chains or in additional cross-linking [15]. The first process softens the polymer and decreases its glass transition temperature and Young's modulus (E) whereas the second process increases T_g and E. Our data indicate that cross-linking prevails at both the vacuum and air conditions.

The observed changes in the mechanical characteristics of the MC can explain parametric variations in the voltage reference microcircuits displayed in Figure 7. It was shown [18] that precision bandgap voltage reference microcircuits are very sensitive to mechanical stresses and that an increase in the compressive stresses decreases the output voltage linearly. An increase of the T_g and E during HTS testing caused an increase of compressive stresses, which at room temperature (T_R) can be expressed as:

$$\sigma \sim E \times (\text{CTE}_1 - \text{CTE}_{\text{LF}}) \times (T_g - T_R).$$

Besides, volatilization of MCs results in shrinkage of the packages, thus also increasing compressive stresses in the dice and decreasing the output voltage.

5.2. Mechanism of wire bond degradation.

At high temperatures, molding compounds in PEMs degrade due to both the thermal and thermo-oxidative degradation processes, which result in release of corrosive molecules capable of attacking Au/Al intermetallic compounds at the wire bonds. The thermal decomposition at $T < 250$ °C occurs relatively slowly and evenly in the bulk of the MC, whereas thermo-oxidative decomposition occurs much more quickly, but only in a relatively thin surface layer of MC where free access to air exists.

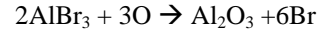
At temperatures below the critical $T < T_c$, the volatile products of the thermo-oxidative degradation from the surface layer of the package are releasing mostly in ambient, and the concentration of the corrosive molecules at the WBs is mostly due to thermal degradation in the bulk of MC and is relatively low. At $T > T_c$, thermal expansion of the MC became large enough resulting in formation of a gap between the lead frame/die assembly and the MC, thus allowing the WBs and adjacent areas of MC free access to air. The thermo-oxidative decomposition of MC in the vicinity of WBs significantly increases the rate of decomposition and concentration of the generated corrosive molecules, thus accelerating degradation of Au/Al intermetallic compounds within and around the wire bonds.

At $T < T_c$, the WB degradation occurs relatively slowly, but with greater activation energy, most likely > 1 eV, which is probably related to the activation energy of the thermal decomposition. At $T > T_c$, the oxidative-decomposition prevails, which accelerates the degradation of WB, but decreases the activation energy of the process, most likely to below 1 eV.

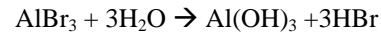
Many authors after Khan [6] believe that diffusion of bromide molecules is the limiting factor in the WB degradation and that the non-linear behavior of the degradation rate near T_g is due to changes in the coefficients of diffusion of these molecules when epoxy polymers transfer from a glassy state to a rubbery state. In this case,

exceeding T_g accelerate transport of the corrosive molecules to the wire bond and thus enhance the rate of degradation. Khan justified his hypothesis based on the fact that the activation energy for Br^- extraction in water (~ 0.8 eV) was similar to the activation energy of WB failures. No other data confirming the diffusion-limiting degradation mechanism was found in relevant literature. Based on our data, it seems more plausible that the rate of generation of corrosive molecules, rather than their diffusivity, is the limiting factor of the degradation process.

Another factor, which might impede WB degradation in vacuum, is related to the deficiency of oxygen. This retards oxidation of aluminum bromide, which is considered as a final stage of the intermetallic corrosion process [5, 7]:



However, decomposition of MC might provide sufficient amount of oxidative molecules, for example, water, which can also react actively with aluminum bromide [6] resulting in degradation of the Au/Al intermetallics:



The following dehydration of aluminum hydroxide at high temperatures will result in formation of aluminum oxide:



Additional experiments and analysis are necessary to elucidate whether the WB degradation in vacuum is limited by these reactions or by the rate of decomposition of MCs.

Microcircuits with silicone die coatings, AD and LT, had 25% to 75% longer mean life times than OP microcircuits. It has been shown [19] that silicones are permeable for volatile halide molecules and do not retard corrosion of Al metallization by the diffusion-barrier mechanism. It is possible, that the effect of silicones is due to their capability to react chemically with the surface of Al, or merely to the fact that the presence of silicone coating increases the distance between the wire bonds and MC thus facilitating removal of the generated corrosive molecules from the package and reducing their concentration at the Au/Al wire bonds. However, more experiments are required to confirm these hypotheses.

6. CONCLUSION

1. The characteristic lifetimes of parametric failures of the three types of PEMs during HTS testing correlated fairly well with the characteristic life times of the WB contact resistance failures, thus confirming that the WB degradation limits reliability of PEMs at high temperatures.
2. The forward voltage drop measurements technique has been shown to be an effective means for evaluation of degradation of WB contact resistance during high-temperature storage testing.
3. Accelerated storage life testing of three types of PEMs at 210 °C in air and vacuum conditions showed that the lifetime in vacuum is 3 to 8 times greater than in air, thus indicating a significant role of oxygen in the high temperature degradation processes in wire bonds.
4. High-temperature storage increases the T_g of MCs in both vacuum and air conditions, and enhances compressive stresses in dice, resulting in a negative shift of the output voltage in precision voltage reference microcircuits.

5. The suggested mechanism of WB degradation at high temperatures explains the existence of a certain critical temperature above T_g , which changes the rate of WB failures by formation of a gap between the MC and the lead frame/die assembly at $T > T_c$. The presence of the gap facilitates access of oxygen to the areas of the MC in the vicinity of WBs, thus accelerating decomposition of the MC and increasing concentration of the volatile corrosive molecules attacking Au/Al intermetallic compounds in the bond.
6. Results of this study indicate the necessity of considering ambient conditions for adequate predictions of reliability of PEMs based on accelerated high-temperature testing. Performing storage testing in a vacuum chamber at temperatures above T_c might allow achieving high acceleration of the WB degradation processes without introducing new failure mechanisms caused by the thermo-oxidative decomposition of MCs.

7. ACKNOWLEDGEMENT

This work was sponsored by the GSFC projects and NASA Electronic Parts and Packaging (NEPP) program. The author would like to thank Darryl Lakins, Head of Code 562, for support of this work. The author also would like to acknowledge Naren Noolu from the Ohio State University, for the opportunity to review his manuscripts, Frederick Felt from QSS Group, Inc., for reviewing the manuscript, Heng Ngien, who carried out most electrical measurements for this work, and Jeanne Beatty for editing this paper.

8. REFERENCES

- [1] G. Harman, "Wire bonding in microelectronics. Materials, Processes, Reliability, and Yield", second edition, McGraw-Hill, 1997.
- [2] N. Noolu, N. Murdeshwar, K. Ely, J. Lippold, W. Baeslack, "Phase transformations in thermally exposed Au-Al ball bonds", *Journal of Electronic Materials*, 2004, in print.
- [3] N. Noolu, N. Murdeshwar, K. Ely, J. Lippold, W. Baeslack, "Partial diffusion reactions and the associated volume changes in thermally exposed Au-Al ball bonds", *Metallurgical and Materials Transactions*, 2004, in print.
- [4] D. Tracy, L. Nguyen, R. Giberti, A. Gallo, C. Bischof, J. Sweet, A. Hsia, "Reliability of aluminum-nitride filled mold compound". *Proceedings 47th Electronic Components and Technology Conference*, 1997, pp. 72 - 77.
- [5] K. Ritz, W. Stacy, E. Broadbent, "The microstructure of ball bond corrosion failures", *IRPS*, 1987, pp. 28-33.
- [6] M. Khan, H. Fatemi, J. Romero, E. Delina, "Effect of high thermal stability mold material on the Au-Al bond reliability in epoxy encapsulated VLSI devices", *26th Annual Proceedings of the International Reliability Physics Symposium*, 1988, pp. 40-49.
- [7] T. Uno, K. Tatsumi, "Thermal reliability of gold-aluminum bonds encapsulated in bi-phenyl epoxy resin, *Microelectronics reliability*, 40, 2000, pp. 145-153.
- [8] A. Gallo, "Effect of mold compound components on moisture-induced degradation of gold-aluminum bonds in epoxy encapsulated devices", *28th Annual Proceedings of the International Reliability Physics Symposium*, 1990, 27-29 Mar, 1990, pp. 244 -251.
- [9] A. Gallo, "Effectors of high temperature reliability in epoxy encapsulated devices", *Proceedings of the 43rd Electronic Components and Technology Conference*, 1993, 1-4 Jun 1993, pp. 356-366.
- [10] M. Tant, H. McManus, M. Rogeers, "High temperature properties and applications of polymeric materials", ACS Washington, DC 1995.
- [11] A. Teverovsky, "In-situ Measurements of Thermo-Mechanical Characteristics of Molding Compounds in PEMs", 2003 International MIL & Aerospace/Avionics COTS conference, Newton-Mariott, Newton, MA, August 27-29, 2003. http://nepp.nasa.gov/index_nasa.cfm/477/
- [12] R. Lowry, K. Hanley, R. Berriche, "Effects of temperatures above the glass transition on properties of plastic encapsulant materials", 7th Intern. Symp. Advanced Packaging Materials, Braselton GA March 11-14, 2000, pp. 57-62.
- [13] R. Biddle, "Plastic Encapsulant Impact on Au-Al Ball Bond Intermetallic Life", http://focus.ti.com/pdfs/mltry/Plastic_Encapsulant_Impact_on_AuAl_Ball_Bond_Intermetallic_Life.pdf
- [14] H. Mark, "Degradation of polymers in hostile environments", 'The effect of hostile environments on coatings and plastics', editors D. Garner, G. Stahl, ACS, Washington D.C., 1983, pp.11-16
- [15] G. Wypych, "Handbook of Material Weathering (2nd Edition), 1995; ChemTec Publishing, pp. 322-328.
- [16] T. Tsotsis, S. Keller, J. Bardis, J. Bish, "Preliminary evaluation of the use of elevated pressure to accelerate thermo-oxidative aging in composites", *Polymer Degradation and Stability*, V. 64, # 2, May 1999, pp. 207-212.
- [17] A. Hill, "Positron annihilation lifetime spectroscopy", in M.Tant, H.McManus, M.Rogeers, High temperature properties and applications of polymeric materials, ACS Washington, DC 1995, pp. 63-77.
- [18] A. Teverovsky, "Environmental hysteresis in molding compounds and voltage reference microcircuits encapsulated in plastics", *Proceedings of the 14th European Microelectronics and Packaging conference*, June 23- 25 Fridrichshafen/Germany, 2003, pp. 219-225. http://nepp.nasa.gov/index_nasa.cfm/477/
- [19] A. Teverovsky, "Chlorine contamination diffusion in silicones", *EEE LINKS*, NASA, April 1999, http://nepp.nasa.gov/index_nasa.cfm/477/.